A size-invariant bud-length timer enables robustness in yeast cell size control

Corey A.H. Allard[1,2*], Franziska Decker[1,3*], Orion D. Weiner[1,4], Jared E. Toettcher[1,5], and Brian R. Graziano[1,4]

[1]Marine Biological Laboratory, Woods Hole, MA
[2]Dept. of Biochemistry and Cell Biology, The Geisel School of Medicine at Dartmouth, Hanover, NH 03755
[3]Max Planck Institute for the Physics of Complex Systems, Max Planck Institute of Molecular Cell Biology and Genetics, Center for Systems Biology Dresden, Dresden, Germany
[4]Cardiovascular Research Institute and Dept. of Biochemistry and Biophysics, UC San Francisco
[5]Department of Molecular Biology, Princeton University, Princeton, NJ

*Equal contribution

Corresponding Authors:
Brian Graziano
University of California, San Francisco
Cardiovascular Research Building, Room 384, MC 3120
555 Mission Bay Blvd. South
San Francisco, CA 94158
Tel. 415-514-4352
brian.graziano@ucsf.edu

Jared Toettcher
Lewis Thomas Laboratory Room 140
Washington Road
Princeton, NJ 08544
Tel. 609-258-1894
toettcher@princeton.edu

Orion Weiner
CVRI & Department of Biochemistry and Biophysics
University of California, San Francisco
Cardiovascular Research Building, Room 352F, MC 3120
555 Mission Bay Blvd. South
San Francisco, CA 94158
Tel. 415-514-4352, Fax 415-514-1176
orion.weiner@ucsf.edu

Summary

Precise control of cell size is evident across nearly all forms of life. Many cellular components, including DNA [1] and organelles [2, 3], display a strong positive correlation with cell size, and maintenance of uniform size may underlie the efficient functioning of tissues and organs [4]. Prior work has uncovered numerous size control strategies operating at different cell cycle stages, but it is less clear how each contributes to the overall size control program. It is also unknown how robust each control system is to large perturbations in cell volume. Since unperturbed cells proliferating in nutrient-rich environments typically grow less than twofold from birth to division, addressing the robustness of size control mechanisms requires a means of acutely perturbing growth to dramatically alter this size distribution. Here, we employed an optogenetic system to reversibly block cell polarization and division in budding yeast. While blocked, cells continued to grow isotropically, increasing in volume by up to 30-fold over unperturbed cells. Upon release, these 'giant' yeast began to proliferate and the population returned to its initial volume distribution. Size control in unperturbed yeast was consistent with an 'adder' mechanism, as previously described [5, 6], where cells add a constant volume between division events. In contrast, this 'adder' failed to explain our observations in giant yeast and volume regulation was instead better described by an invariant bud growth 'timer'. Our results indicate that yeast size control arises from distinct mechanisms that employ both size sensors and timers to ensure a uniform volume distribution.

RESULTS AND DISCUSSION

Optogenetics for cell size control. How cells maintain a tight distribution of sizes as they proliferate has been a long-standing question, and previous studies have offered several major classes of models to account for this phenomenon. These include the 'sizer' (progression through the cell cycle is triggered above a specified cell size), 'adder' (cells add a constant volume increment over the course of one cell cycle), and 'timer' (duration of a cell cycle phase is specified independently of cell volume) [7–12]. In budding yeast (*S. cerevisiae*), previous work has shown that individual yeast in unperturbed populations of cells grow exponentially in size [5, 13, 14], and theoretical studies have shown that exponential growth will cause cell sizes in a population to diverge unless cells are able to measure their size and regulate cell cycle progression accordingly [4, 12, 15, 16]. Consistent with this idea, volume regulation in yeast relies on the molecular size-sensor Whi5 [17] and overall growth appears to be well-described by an adder model in which cells increase by a constant volume between budding events [5].

Although overall size scaling relationships in yeast, bacteria and mammalian cells are well-described by the adder model [18–22], important questions remain about how cell size control is implemented and the range of sizes over which it can function. Even a single observed scaling relationship (such as the adder) may rely on distinct mechanisms operating at different cell cycle phases [6, 23, 24]. In budding yeast, distinct growth rates and modes of regulation throughout the cell cycle are especially likely because the geometry of cell growth is highly cell cycle dependent, with isotropic growth occurring during G1 and polarized/budded growth occurring during S/G2. Moreover, it has not been carefully examined how robust cell size control and growth rate are to large variations in cell size (**Fig. 1A**). As in the case of cell polarity, redundant mechanisms may act to ensure size control even when individual mechanisms break down [25, 26]. Here, we hypothesized that the ability to prepare yeast across a broad range of cell sizes would enable us to decouple the action of different growth and size-control programs and probe their robustness to large variations in size (**Fig. 1A**).

To achieve reversible control over cell size in *S. cerevisiae*, we took advantage of a recently-described system using light-responsive phytochrome proteins to control the activity of Bem1, a cell polarity factor [27, 28]. When illuminated with red light, Bem1 is anchored away to the mitochondria and its activity on the plasma membrane is disrupted. Under these conditions cells fail to form a site of polarized Cdc42 activity and do not undergo bud formation, but instead undergo continuous isotropic growth [27]. Strikingly, this effect is quickly reversed upon illumination with infrared (IR) light: Bem1

is released from the mitochondria, driving immediate polarization, bud formation, and completion of the cell cycle (**Fig. 1B-D**).

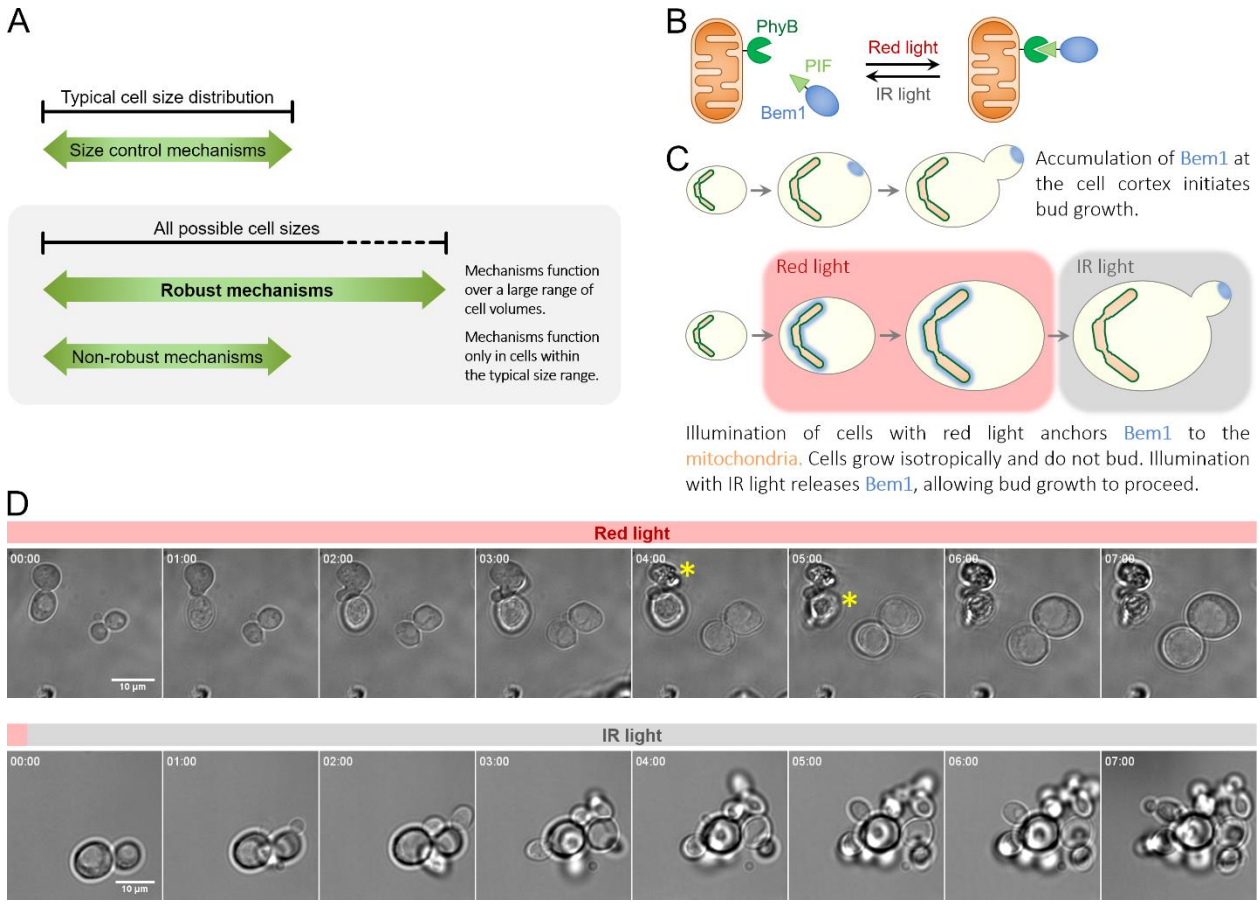

Figure 1. Control of yeast cell size using optogenetics. (A) Schematic depicting robust and non-robust mechanisms for size control. **(B)** Exogenous PhyB (phytochrome B; dark green) is fused to the C-terminus of *S. cerevisiae* Tom20, anchoring it to the mitochondria outer membrane (orange). PIF (phytochrome-interacting factor; light green) is fused to endogenous Bem1 (blue). Illumination with red light drives a conformational change in PhyB allowing it to bind PIF-Bem1. Conversely, illumination with infrared (IR) light drives the reverse reaction, releasing PIF-Bem1. **(C)** Top row. Bem1 (blue) localization to the plasma membrane is required for bud emergence and polarized growth. Bottom row. Illumination of yeast with red light sequesters Bem1 to the mitochondria (orange), preventing it from localizing to the plasma membrane to initiate budding. Yeast continue to grow isotropically while under red light. Illumination of yeast with IR light releases Bem1 from the mitochondria, allowing it to promote budding. **(D)** Top row. Cells were illuminated with red light for 8 h and imaged every 10 min using bright-field microscopy. Yellow asterisks indicate cells undergoing lysis. Bottom row. Following red light illumination for 6-10 hours, large cells were illuminated with IR light and imaged every 5-10 min using bright-field microscopy.

Isotropic growth in giant yeast is proportional to surface area. We first used our optogenetic system to decouple isotropic from polarized growth by continuously illuminating yeast with red light to deactivate Bem1. As yeast became increasingly large, they began to lyse (e.g., **Fig. 1D**, yellow asterisks), as we previously reported [27]. To provide osmotic balance and counteract this effect, we grew yeast in media containing 1 M sorbitol. These conditions increased yeast survival (**Fig. 2A**) without affecting the rate of isotropic growth (**Fig. 2B**); we therefore supplemented our media with sorbitol for all subsequent experiments. Performing a pulse-chase experiment with fluorescent concanavalin-A validated that growth was indeed isotropic during the entire time period, with fluorescence evenly diluted across the cell surface and maintenance of a spherical cell shape (**Fig. 2C**). Over a period of 6 hours of isotropic growth, yeast increased in volume by as much as 30-fold (**Fig. 2D**). Growth rates in Bem1-deactivated cells appeared to be cell cycle-dependent since asynchronous and synchronized cells displayed bimodal and unimodal rates of growth, respectively (**Figs. 2B and S1A-B**). Most cells exhibited a ploidy of 2N or less throughout isotropic growth (**Fig. 2E-F**). Yeast also appeared to exhibit a linear relation between protein levels and cell volume over their entire size distribution (**Fig. S1C**) as assessed by protein fluorescence [13].

Cells typically undergo less than a twofold change in volume as they proliferate and distinguishing between cell growth laws over this narrow range requires precise volume measurements (e.g. for linear vs. exponential growth, a measurement error of less than 6%) [29]. In contrast, the much broader range of sizes of Bem1-deactivated cells led to highly divergent predictions between different growth laws (**Fig. 2D**). Surprisingly, we found that in isotropically-growing yeast the rate of volume increase was neither linear nor exponential. Rather, cells added volume in proportion to their surface area, a growth law that can be easily identified by a linear change in cell diameter with time (**Fig. 2D**; see Supplemental Experimental Procedures). While this result would appear to conflict with previous studies indicating exponential growth in yeast [5, 13], the rate of yeast growth exhibits cell cycle dependence [30] and unperturbed cells gain the vast majority of their volume during polarized bud growth (during S/G2). Here, we specifically measure cellular volume increases during isotropic growth in G1, which may be subject to distinct growth control laws. It is also possible that exponential growth operates over the limited volume range of unperturbed cells and quickly breaks down as nutrient exchange across the plasma membrane becomes limiting for growth [31].

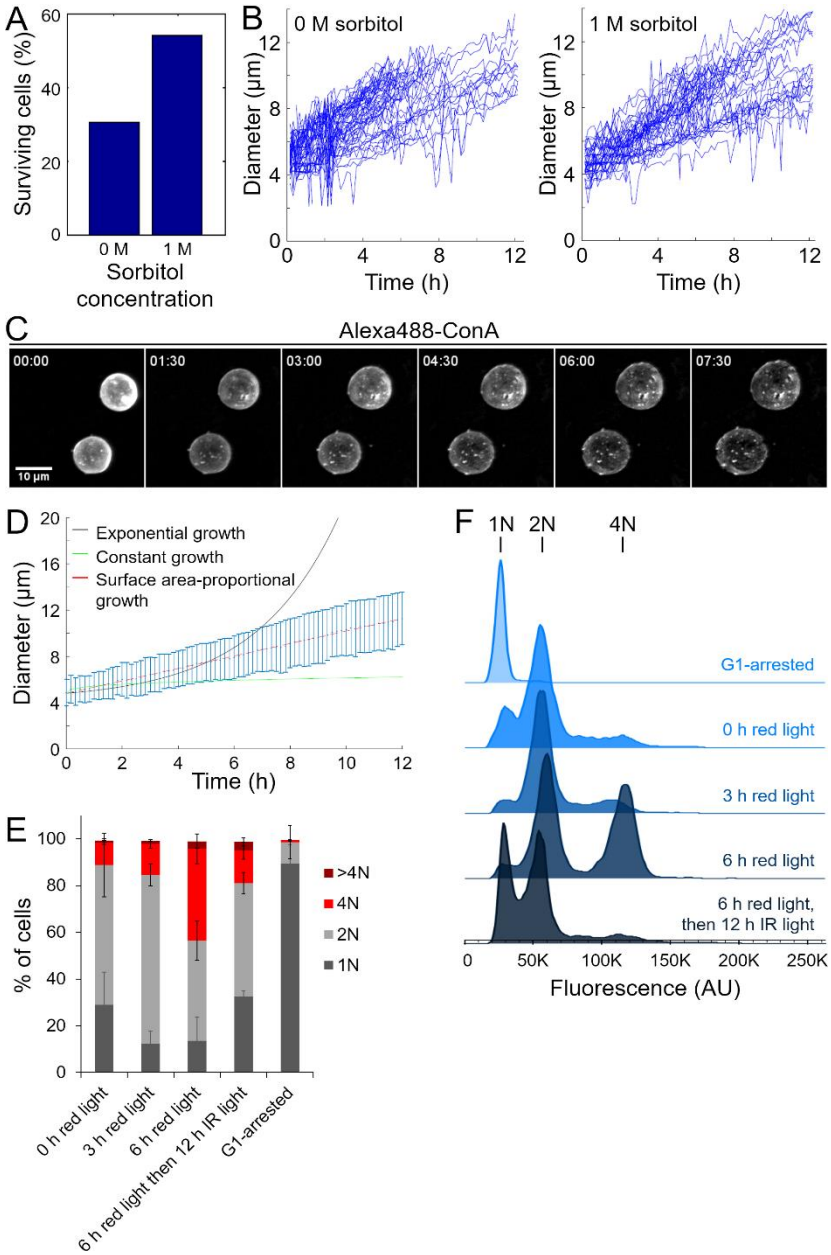

Figure 2. Effects of continuous isotropic growth on yeast physiology. (A) Yeast were prepared and imaged as in **Fig. 1D** with media containing indicated concentrations of sorbitol. Each bar indicates the percentage of cells surviving the entire 10-h timecourse. **(B)** Single cell growth curves of yeast from experiment described in 2A with or without 1 M sorbitol. **(C)** Cell wall staining. Cells were prepared as in 2A, treated with 100 µg/mL Alexa488-labeled concanavalin-A, and imaged every 15 min for 8 h. Each panel is a max intensity projection of multiple focal planes acquired via confocal microscopy. Yeast grow isotropically during Bem1 deactivation. **(D)** Average growth rates calculated as in 2B for yeast in 1 M sorbitol from experiments described in 2A. Each blue dot represents an average of 48 cells. Expected trajectories for exponential, constant, and surface-area-proportional growth are indicated by black, green, and red lines, respectively. Error bars, SD. **(E)** Cells were treated with red light for 6 h, followed by an additional 12 h of IR light. Cells were fixed and stained with SYTOX Green at indicated timepoints following treatment. 'G1-arrested' cells were treated with alpha-factor for 3 h to arrest cells in G1, with a ploidy of 1N. **(F)** Representative plots from flow cytometry experiments depicted in 2E. Ploidy was determined by performing control experiments in parallel with G1-arrested cells. The mean SYTOX green fluorescence in these control samples was used as a standard for determining ploidy in all experimental samples.

The adder model for size control breaks down as cell volume becomes increasingly large. Recent work has demonstrated that size regulation in unperturbed yeast operates via an apparent adder, with a constant volume increase between two sequential budding events [5] (**Fig. 3A**). This adder model stipulates that (i) above-average growth during G1 should be offset by below-average growth in S/G2, and vice-versa, and (ii) the duration of S/G2 (i.e. budding) is size-invariant [5]. Given these constraints, an adder could only maintain uniform size in increasingly large mothers if the growth rate during S/G2 could be reduced. If not, there would exist a critical volume beyond which bud volume increases during S/G2 would exceed the entire volume increment allotted to each cell cycle (i.e., the above-average volume increase during S/G2 could not be offset during G1 since growth cannot be negative) and the adder would fail.

To test whether the adder fails as cells grow beyond this critical volume, we generated cells with volumes spanning a >10-fold range by using our optogenetic system to deactivate Bem1 in yeast for 8 h. We then reactivated Bem1 by illuminating cells with IR light and observed cell growth through successive rounds of birth/division. To precisely time the beginning and end of budding, we observed the dynamics of fluorescently-labeled septin rings [32] (**Fig. 3B**). For unperturbed cells, volume at division correlated linearly with volume at birth with a slope of 1.19 (95% CI, 0.82-1.56) (**Fig. 3C**), in close agreement with previous work showing that yeast near their normal size range regulate volume using an apparent adder, which would correspond with a slope of 1 [5]. In contrast, we found that the adder model poorly explained the cell size relationships in our giant cells. This discrepancy was evident in at least two observations: cell volume at division was related to cell volume at birth with a slope of 1.73 (95% CI, 1.32-2.13) [5] (**Fig. 3C**); and the change in volume from birth to division (i.e. the volume increment specified by the adder) was not constant, but rather positively correlated with the cell's birth volume (**Fig. 3D**).

Together, our data indicate that cells within their typical size range are well-described by an apparent adder where volume changes during S/G2 can be effectively offset by compensatory volume changes during G1 (**Fig. 3E**, "Typical size"). However, there also exists a critical volume beyond which G1 can no longer compensate for large volume increases during S/G2. The unrestricted bud growth our conceptual model predicts would then drive a larger-than-expected volume addition per cell cycle (**Fig. 3E**, "Giant size").

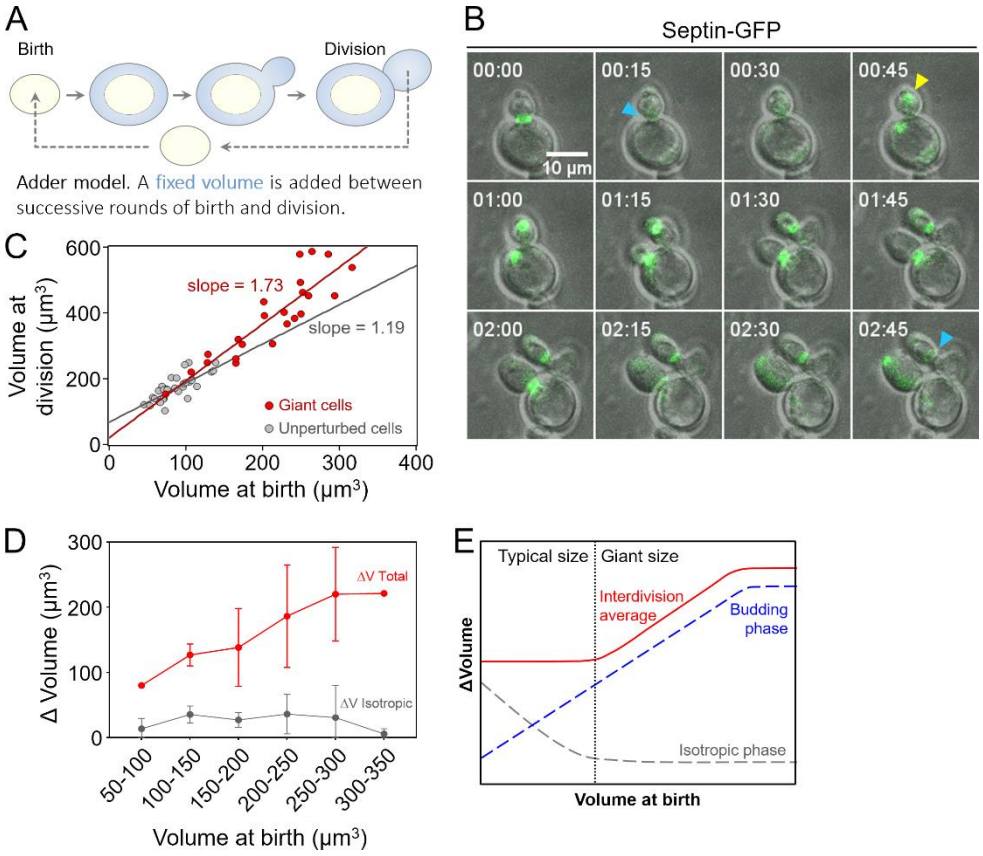

Figure 3. Adder-based size control is not observed in giant yeast. (A) Schematic depicting adder-based growth in budding yeast. **(B)** Cells were illuminated for 8-10 h with red light (to generate giant yeast), then switched to IR light (allowing giant yeast to bud and divide) and imaged every 5 min for ~8 h. Exogenously-expressed Cdc10-GFP was used to mark septin rings (green). Birth and division were marked by successive rounds of septin ring disappearance (blue arrows). Bud emergence was marked by septin ring appearance (yellow arrows). **(C-D)** Cells were imaged and analyzed as depicted in 3B. 'Volume at birth' for daughters was measured when the septin ring separating the mother and daughter disappeared (e.g., '00:15' in 3B). 'ΔV Isotropic' is the difference between volume measured when bud emergence occurred in newly-born daughters (e.g., '00:45' in 3B), and 'Volume at birth'. 'Volume at division' was measured when daughters completed a subsequent round of cytokinesis (e.g., '02:45' in 3B) and included both the original daughter and her newly-formed bud. 'ΔV Total' is the difference between 'Volume at division' and 'Volume at birth'. **(C)** Each point represents a single cell. Grey and red lines, best-fit line by linear regression analysis for either unperturbed or giant cells, respectively. **(D)** Cells were binned by volume at birth, as indicated. N = 28 cells. **(E)** Schematic depicting relations between the volume added during the isotropic growth phase (G1) and budded growth phase (S/G2) for an adder growth mechanism in unperturbed cells ('Typical size') vs. our observations for increasingly larger cells ('Giant size').

A 'timer' specifying budding duration operates across a broad range of cell sizes. If an 'adder' is unable to explain the S/G2 growth observed in giant yeast, what growth laws and size control mechanisms might operate in this regime? We and others envisioned two possibilities: a bud 'sizer', in which cytokinesis would commence upon the bud reaching a critical volume to limit bud size in giant mothers; and a bud 'timer' in which cytokinesis would occur after a fixed amount of time from the initiation of budding (**Fig. 4A**). To distinguish between these possibilities, we tracked the timing of bud emergence and division by the appearance and disappearance of septin rings, respectively (**Fig. 4B**). We found that daughter volume strongly correlated with mother volume (**Fig. 4C**), inconsistent with a bud 'sizer' mechanism. Our prior observation that volume addition over a cell cycle scales positively with cell birth size (**Fig. 3D**) further argues against a bud 'sizer' for cell volume control. In contrast, our data was consistent with a timer mechanism: Budding duration (the time from bud emergence to division) showed no correlation with mother cell volume and took on average 95 min across cells of all volumes (**Fig. 4D**). These results agree with several earlier studies showing that budding duration in yeast is generally invariant [5, 33, 34]. Our own observations thus extend these previous findings by demonstrating that this fixed 'timer' for bud growth also operates in yeast more than an order of magnitude larger than their typical volume range.

The absence of a robust adder operating in giant yeast might be expected to interfere with the return to an unperturbed size distribution after Bem1 reactivation. To address this question, we measured cell size as a function of time following reactivation of Bem1 in giant cells using IR light. Surprisingly, we found that the cell population rapidly returned to its unperturbed state (**Fig. 4E**). Individual daughter cells reached their pre-stimulation volume in as few as three rounds of division (**Fig. S2**). This return to their typical size is not driven by cell shrinking: giant mothers maintained their maximum size over multiple rounds of budding (e.g., **Fig. 1D**, bottom row). Taken together, our results demonstrate that the combination of sub-exponential growth of large cells and a timer specifying the duration of budding serves as a highly robust size control system for driving cell volumes down to their appropriate range.

In sum, we find that the apparent adder describing size control in unperturbed yeast is not operational in giant cells. Since the adder's proper functioning depends on compensatory volume additions in G1 and S/G2 [5], the breakdown of this mechanism in giant yeast likely arises from size-dependent growth during the fixed duration of budding, combined with an already minimal amount of growth in the subsequent G1 phase (e.g., **Fig. 3D**, grey curve). Nevertheless, these enlarged yeast do

retain the ability to converge on their set-point volume following successive rounds of division (**Fig. 4E**). This behavior relies primarily on two features of scaling and size control: (i) a sub-exponential growth rate limiting volume addition in giant cells, and (ii) a size-invariant timer governing the duration of the budded period during S/G2 (**Fig. 4D**). Convergence of giant yeast to their unperturbed size may also be aided by an apparent upper-limit on daughter cell volume: While daughter volume generally scales with mother volume, mothers larger than ~700 μm^3 produced daughters of uniform volume of ~250 μm^3 (**Fig. 4C**). This cap on daughter cell volume may represent a physical limit to the rate of bud growth (e.g. an upper limit on the rate of secretory vesicle transport through the bud neck) [35]. Our results suggest that maintenance of a constant time between bud emergence and division is sufficient to ensure that cells never become too large, while molecular size sensors controlling progression to START, such as Whi5 [17], are required for specifying a minimum cell volume. As our optogenetic-based approach is both acute and reversible, it represents a significant advance over established methods for perturbing cell size (e.g. gene deletion or *ts* alleles), where pleiotropic effects or environmental stress may influence volume regulation and complicate analysis. We anticipate that such tools will constitute an important new strategy for addressing other questions related to cell size control, including those involving the relationship between organelle size and cell volume.

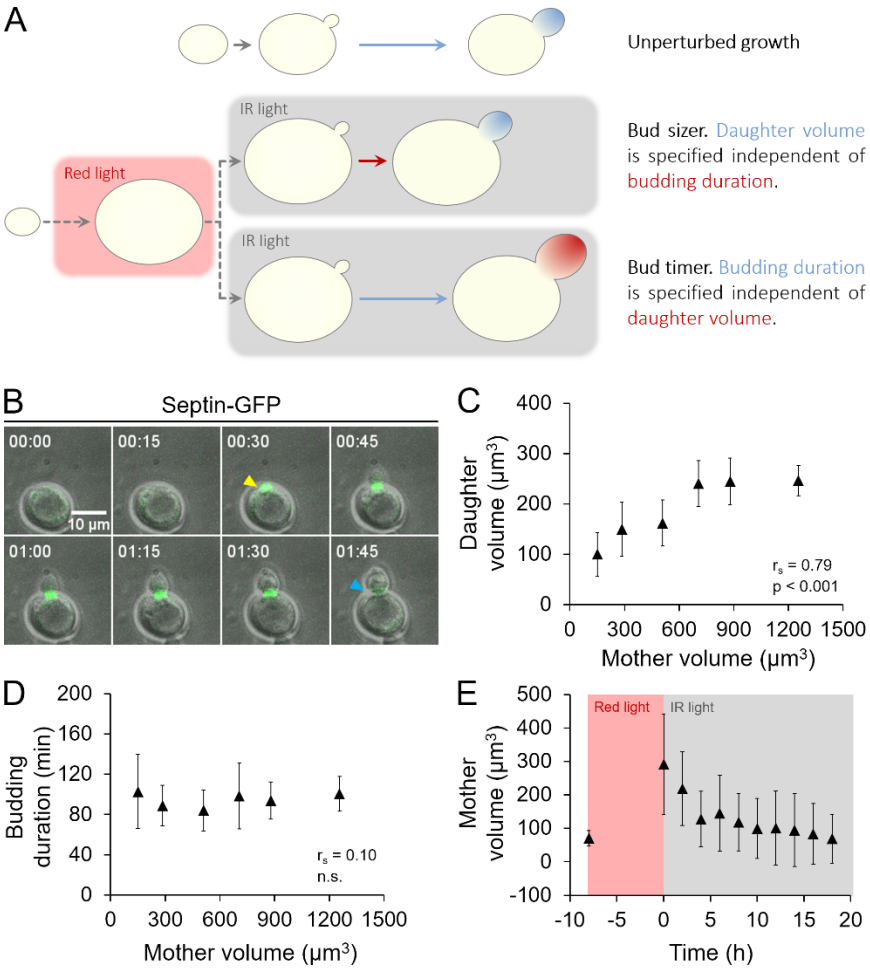

Figure 4. Comparison of sizer and timer mechanisms for regulation of bud growth. (A) Schematic depicting the use of our optogenetics system for discriminating between bud 'sizer' and bud 'timer' mechanisms for specifying daughter cell volume. **(B)** Cells were illuminated for 6-8 h with red light (to generate giant yeast), then switched to IR light (allowing giant yeast to bud and divide) and imaged every 5 min for ~8 h. Exogenously-expressed Cdc10-GFP was used to mark septin rings (green) as in 3A. **(C and D)** Cells were imaged and analyzed as depicted in 4B. Cells were binned by mother volume in 200-µm increments. The average volume within each bin is plotted. Budding duration, difference between the time of division (e.g., '01:45' in 4B) and time of birth (e.g., '00:30' in 4B). 'Mother volume' was measured at the time of daughter cell birth (e.g., yellow arrow in 4B); 'daughter volume' was measured at cytokinesis (e.g., blue arrow in 4B). N = 73 cells, with each bin containing at least 5 cells. Error bars, SD. r_s, Spearman's rho. **(E)** Cells were incubated under red light illumination for 8 h followed by IR light illumination for 18 h. At indicated timepoints, cell volumes were measured by microscopy as in C-D. Each point represents an average of >80 cells. Error bars, SD.

MATERIALS AND METHODS

Strains, plasmids, and growth conditions. All yeast strains used are isogenic to an 'opto-Bem1' strain which was created in the w303 genetic background and contained exogenous PhyB-mCherry-Tom7 with endogenous Bem1 C-terminally tagged with mCherry-PIF, as previously described [27]. A pACT1-CDC10-eGFP expression vector was created by Gibson assembly [36], with the CDC10 expression cassette inserted between the NotI and XmaI sites of the pRS316 vector [37]. For the experiments described in **Fig. 2D** and **Figs. 3-4**, the indicated vector was transformed into our opto-Bem1 strain and selection was maintained by growing yeast in synthetic complete media lacking uracil (Sunrise). For all other experiments, yeast were cultured in synthetic complete media (Sunrise).

Preparation of yeast for optogenetic experiments. Preparation of yeast prior to optogenetic experiments was performed, in general, as previously described [27]. Yeast undergoing exponential growth in synthetic media (with or without 1 M sorbitol) were treated with 31.25 µM phycocyanobilin (PCB; Santa Cruz Biotechnology, Inc.) and incubated in foil-wrapped tubes (to block light) at 30 °C for a minimum of 2 h. For all microscopy experiments, yeast were spun onto glass-bottom 96-well plates (Brooks) coated with Concanavalin A and washed once with fresh PCB-containing media (with or without sorbitol) to remove floating cells. Cells remained approximately spherical following this procedure, as assessed by Concanavalin A staining (e.g., **Fig. 2C**). Mineral oil (Sigma-Aldrich) was then carefully layered on top of each sample to prevent evaporation. Imaging was performed at room temperature. For experiments where isotropic growth was measured (e.g., **Fig. 2A**), yeast were plated and imaged immediately following PCB treatment. For experiments where growth following Bem1 reactivation was examined (e.g., **Fig. 3**), PCB-treated yeast were first placed in clear culture tubes and incubated at room temperature for >6 h while undergoing constant illumination with a red LED panel (225 Red LED Indoor Garden Hydroponic Plant Grow Light Panel 14W, HQRP). Cells were then plated and imaged.

Microscopy. For isotropic growth experiments, samples were imaged on a Nikon Eclipse Ti inverted microscope equipped with a motorized stage (ASI), a Lamba XL Broad Spectrum Light Source (Sutter), a 60x 1.4 NA Plan Apo objective (Nikon), and a Clara interline CCD camera (Andor). For the remaining experiments, samples were imaged on one of two spinning disk confocal microscopes, both of which were Nikon Eclipse Ti inverted microscopes with motorized stages (ASI). The first microscope was equipped with a Diskovery 50-µm pinhole spinning disk (Spectral Applied Research), a laser merge

module (LMM5, Spectral Applied Research) with 405, 440, 488, 514, and 561-nm laser lines, a 60x 1.49 NA TIRF Apo objective (Nikon), and a Zyla sCMOS camera (Andor). The second microscope was equipped with CSU-X1 spinning disk (Yokugawa), a MLC400B monolithic laser combiner (Agilent) with 405, 488, 561, and 640-nm laser lines, a 60x 1.4 NA Plan Apo objective (Nikon), and a Clara interline CCD camera. All microscopes were controlled using Nikon Elements.

For isotropic growth experiments, samples were imaged by bright-field microscopy every 10 min for 12 h. Throughout the experiment a red LED panel (HQRP) was carefully balanced against the motorized stage and microscope body to provide oblique illumination to the cells and ensure that Bem1 remained deactivated. Generous amounts of lab tape (Fisher) were applied to the LED panel and scope to prevent slippage during image acquisition and stage movement.

For experiments where Bem1 was reactivated following >6 h of deactivation, images were acquired every 5-10 min. During imaging, a 725-nm longpass filter (FSQ-RG9, Newport) was placed in the transmitted light path (gently resting on top of the condenser). The shutter for the transmitted light source was then left open for the entire duration of the experiment (even when images were not actively being acquired), such that cells were constantly illuminated with IR light, ensuring that Bem1 remained 'activated'. However, the shutter was briefly closed during acquisition of Cdc10-GFP images to reduce background.

Image Analysis. Cell volumes for yeast undergoing isotropic growth (i.e., **Figs. 2B, D and S1A-B**) were measured using custom Matlab code where a Hough transform was applied to bright-field images to identify cell boundaries. Cell radii were determined by calculating the geometric mean of the major and minor axes of the resulting ellipse. For cells growing and dividing following Bem1 release (i.e., **Figs. 3C-D, 4C-E, and S2**) cell volumes were calculated by manually fitting ellipses to the cell boundaries within a single focal plane passing through the center of the cell. The major and minor axes of the ellipses were then determined, and cell volumes were calculated by solving for the volume of a prolate spheroid. For analysis of bud 'sizer' and bud 'timer' mechanisms (**Fig. 4C-D**), we included in our analysis mother cells that had previously been Bem1-deactivated. These cells were omitted from our analysis of total volume addition over the course of an entire cell cycle (**Fig. 3**), given that we had strongly perturbed their growth during G1 via Bem1 deactivation. Inclusion of these cells also significantly increased the volume range of mother cells for which we could measure daughter cell volumes.

Quantification of protein levels. To determine cellular protein levels in growing yeast, we quantified mCherry fluorescence in our cells, which expressed *BEM1-mCherry-PIF* under the endogenous *BEM1* promoter and *PhyB-mCherry-CAAX* under the *ADH1* promoter, by spinning-disc confocal microscopy. Isotropic growth was induced as described in the "Preparation of yeast for optogenetic experiments" section. Cells were imaged 6 h following optogenetic-based Bem1 deactivation. Z-stacks containing 51 slices with 0.5 µm spacing with the shutter remaining open between each z-step were then collected. Sum projections were created from the entire stack, corrected for uneven illumination, and processed to remove background. Fluorescence intensity was measured from whole-cell regions-of-interest using ImageJ. Cell volume was approximated by measuring the major and minor axis of each cell and using these values to solve for the volume of an prolate spheroid.

Flow cytometry to measure ploidy. PCB-treated cells were placed in clear culture tubes and incubated at room temperature while undergoing constant illumination with a red LED panel. Samples (200 µL each) were collected at 0, 3, and 6 h following illumination with red light. The remainder of the culture was then placed under an IR LED (740-nm, Lightspeed Technologies) for an additional 12 h, after which a final sample was collected. Upon collection, cells were immediately treated with 475 µL 100% ethanol and fixed for 1 h at room temperature. Cells were then pelleted, washed once with 50 mM sodium citrate (pH = 7.2), and then resuspended in 500 µL 50 mM sodium citrate (pH = 7.2) to which RNaseA (0.25 mg/mL) had been added. Following an incubation for 1 h at 37 °C, 50 µL proteinase K was added to a final concentration of 2 mg/mL and cells were incubated at 50 °C for an additional hour. SYTOX green was then added to each sample to a final concentration of 2 µM, and cells were incubated for 1 h at room temperature. In parallel, control samples were prepared containing exponentially growing cultures of yeast treated with α-factor (10 µg/mL) for for ~3 h prior to fixation and staining. Ploidy was determined by measuring the fluorescence intensity of SYTOX green staining by flow cytometry using a FACSAria III (BD Biosciences) and normalizing to the α-factor-treated samples, which have a ploidy of 1N. Analysis of flow cytometry data was performed using FlowJo and Flowing Software (http://flowingsoftware.btk.fi).

ACKNOWLEDGEMENTS

We thank Anna Payne-Tobin Jost for helpful discussions, Alba Diz-Muñoz for experimental assistance, Fred Chang for critical reading of the manuscript and Nairi Hartooni for reagents. We also thank the organizers of the 2015 MBL Physiology course, Wallace Marshall, Jennifer Lippincott-Schwartz, and Rob Phillips, as well as all the course staff for creating the well-run, intellectually-stimulating environment from which this project grew. Support for this work was provided by a Post-Physiology Course Award from the Marine Biological Laboratory (CAHA), the Thomas B. Grave and Elizabeth F. Grave Scholarship (FD), NIH GM118167 (ODW), NIH DP2EB024247 (JET), and NIH T32HL773125 (BRG).

REFERENCES

1. Gregory, T. R. (2001). Coincidence, coevolution, or causation? DNA content, cell size, and the C-value enigma. Biol Rev Camb Philos Soc *76*, 65–101.
2. Marshall, W. F. (2011). Origins of cellular geometry. BMC Biol *9*, 57.
3. Goehring, N. W., and Hyman, A. A. (2012). Organelle growth control through limiting pools of cytoplasmic components. Curr Biol *22*, R330–9.
4. Ginzberg, M. B., Kafri, R., and Kirschner, M. (2015). Cell biology. On being the right (cell) size. Science *348*, 1245075.
5. Soifer, I., Robert, L., and Amir, A. (2016). Single-Cell Analysis of Growth in Budding Yeast and Bacteria Reveals a Common Size Regulation Strategy. Curr Biol *26*, 356–361.
6. Chandler-Brown, D., Schmoller, K. M., Winetraub, Y., and Skotheim, J. M. (2017). The Adder Phenomenon Emerges from Independent Control of Pre- and Post-Start Phases of the Budding Yeast Cell Cycle. Curr Biol *27*, 2774–2783.e3.
7. Conlon, I., and Raff, M. (2003). Differences in the way a mammalian cell and yeast cells coordinate cell growth and cell-cycle progression. J Biol *2*, 7.
8. Amir, A. (2014). Cell size regulation in bacteria. Phys. Rev. Lett. *112*.
9. Fantes, P. A. (1977). Control of cell size and cycle time in Schizosaccharomyces pombe. J Cell Sci *24*, 51–67.
10. Johnston, G., Pringle, J., and Hartwell, L. (1977). Coordination of growth with cell division in the yeast. Exp Cell Res *105*, 79–98.
11. Pan, K. Z., Saunders, T. E., Flor-Parra, I., Howard, M., and Chang, F. (2014). Cortical regulation of cell size by a sizer cdr2p. elife *3*, e02040.
12. Lloyd, A. C. (2013). The regulation of cell size. Cell *154*, 1194–1205.
13. Di Talia, S., Skotheim, J. M., Bean, J. M., Siggia, E. D., and Cross, F. R. (2007). The effects of molecular noise and size control on variability in the budding yeast cell cycle. Nature *448*, 947–951.
14. Godin, M., Delgado, F. F., Son, S., Grover, W. H., Bryan, A. K., Tzur, A., Jorgensen, P., Payer, K., Grossman, A. D., Kirschner, M. W., et al. (2010). Using buoyant mass to measure the growth of single cells. Nat Methods *7*, 387–390.
15. Amodeo, A. A., and Skotheim, J. M. (2016). Cell-Size Control. Cold Spring Harb Perspect Biol *8*, a019083.
16. Brooks, R. F., and Shields, R. (1985). Cell growth, cell division and cell size homeostasis in Swiss 3T3 cells. Exp Cell Res *156*, 1–6.
17. Schmoller, K. M., Turner, J. J., Kõivomägi, M., and Skotheim, J. M. (2015). Dilution of the cell cycle inhibitor Whi5 controls budding-yeast cell size. Nature *526*, 268–272.

18. Cadart, C., Monnier, S., Grilli, J., Attia, R., Terriac, E., Baum, B., Cosentino-Lagomarsino, M., and Piel, M. (2017). Size control in mammalian cells involves modulation of both growth rate and cell cycle duration. BioRxiv.

19. Taheri-Araghi, S., Bradde, S., Sauls, J. T., Hill, N. S., Levin, P. A., Paulsson, J., Vergassola, M., and Jun, S. (2015). Cell-size control and homeostasis in bacteria. Curr Biol *25*, 385–391.

20. Campos, M., Surovtsev, I. V., Kato, S., Paintdakhi, A., Beltran, B., Ebmeier, S. E., and Jacobs-Wagner, C. (2014). A constant size extension drives bacterial cell size homeostasis. Cell *159*, 1433–1446.

21. Varsano, G., Wang, Y., and Wu, M. (2017). Probing Mammalian Cell Size Homeostasis by Channel-Assisted Cell Reshaping. Cell Rep *20*, 397–410.

22. Deforet, M., van Ditmarsch, D., and Xavier, J. B. (2015). Cell-Size Homeostasis and the Incremental Rule in a Bacterial Pathogen. Biophys J *109*, 521–528.

23. Delarue, M., Weissman, D., and Hallatschek, O. (2017). A simple molecular mechanism explains multiple patterns of cell-size regulation. PLoS ONE *12*, e0182633.

24. Sveiczer, A., Novak, B., and Mitchison, J. M. (1996). The size control of fission yeast revisited. J Cell Sci *109 (Pt 12)*, 2947–2957.

25. Wedlich-Soldner, R., Wai, S. C., Schmidt, T., and Li, R. (2004). Robust cell polarity is a dynamic state established by coupling transport and GTPase signaling. J Cell Biol *166*, 889–900.

26. Slaughter, B. D., Das, A., Schwartz, J. W., Rubinstein, B., and Li, R. (2009). Dual modes of cdc42 recycling fine-tune polarized morphogenesis. Dev Cell *17*, 823–835.

27. Jost, A. P.-T., and Weiner, O. D. (2015). Probing Yeast Polarity with Acute, Reversible, Optogenetic Inhibition of Protein Function. ACS Synth Biol *4*, 1077–1085.

28. Chenevert, J., Corrado, K., Bender, A., Pringle, J., and Herskowitz, I. (1992). A yeast gene (BEM1) necessary for cell polarization whose product contains two SH3 domains. Nature *356*, 77–79.

29. Tzur, A., Kafri, R., LeBleu, V. S., Lahav, G., and Kirschner, M. W. (2009). Cell growth and size homeostasis in proliferating animal cells. Science *325*, 167–171.

30. Goranov, A. I., Cook, M., Ricicova, M., Ben-Ari, G., Gonzalez, C., Hansen, C., Tyers, M., and Amon, A. (2009). The rate of cell growth is governed by cell cycle stage. Genes Dev *23*, 1408–1422.

31. Turner, J. J., Ewald, J. C., and Skotheim, J. M. (2012). Cell size control in yeast. Curr Biol *22*, R350–9.

32. Cid, V. J., Adamiková, L., Sánchez, M., Molina, M., and Nombela, C. (2001). Cell cycle control of septin ring dynamics in the budding yeast. Microbiology (Reading, Engl) *147*, 1437–1450.

33. Hartwell, L. H., and Unger, M. W. (1977). Unequal division in Saccharomyces cerevisiae and its implications for the control of cell division. J Cell Biol *75*, 422–435.

34. Von Meyenburg, H. K. (1968). Der Sprossungszyklus von *Saccharomyces cerevisiae*. Pathobiology *31*, 117–127.

35. Pruyne, D. W., Schott, D. H., and Bretscher, A. (1998). Tropomyosin-containing actin cables direct the Myo2p-dependent polarized delivery of secretory vesicles in budding yeast. J Cell Biol *143*, 1931–1945.

36. Gibson, D. G., Young, L., Chuang, R.-Y., Venter, J. C., Hutchison, C. A., and Smith, H. O. (2009). Enzymatic assembly of DNA molecules up to several hundred kilobases. Nat Methods *6*, 343–345.

37. Sikorski, R. S., and Hieter, P. (1989). A system of shuttle vectors and yeast host strains designed for efficient manipulation of DNA in Saccharomyces cerevisiae. Genetics *122*, 19–27.

SUPPLEMENTARY MATERIALS

Figure S1. Characterization of optogenetically-induced isotropic growth, related to Figure 2. (A) Cells were prepared as in 2B and synchronized in S-phase via incubation with 0.2 M hydroxyurea for 3 h followed by washout using media containing 1 M sorbitol. **(B)** Probability distributions for growth rates measured in cells from S1C and 2B, right panel. **(C)** Fluorescence of exogenously-expressed PhyB-mCherry-Tom7 under control of an ADH1 promoter was measured in cells of indicated volumes. Cells were binned by mother volume in 200-µm increments. The average volume within each bin is plotted. N = 300 cells. Error bars, SD. r, Pearson's correlation coefficient.

Figure S2. Volume measurements of successive generations of daughter cells, related to Figure 4. Representative daughter cells from experiments in Fig. 4C-D. Only the daughters of daughters were measured for each generation.

Supplemental Experimental Procedures.

Supplemental Figure 1

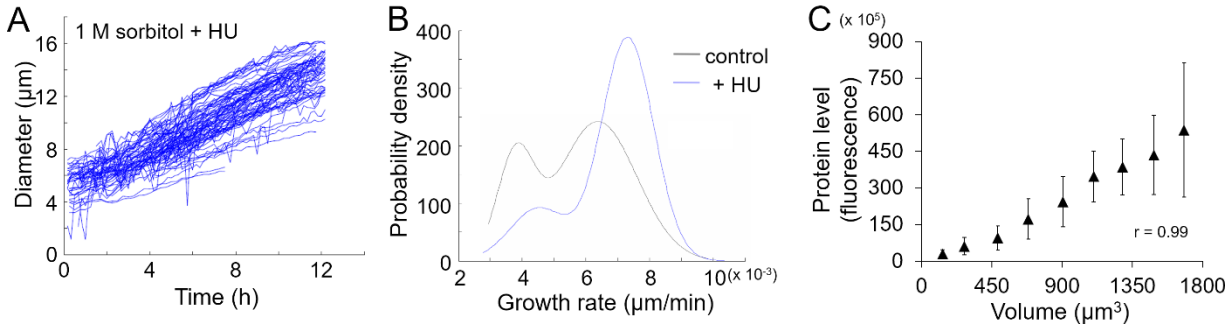

Supplemental Figure 2

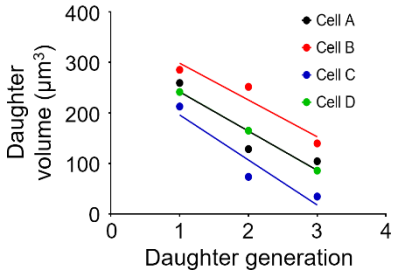

Supplemental Experimental Procedures

1 Different models of growth

1.1 Growth proportional to surface area

We found that the radius r grows linearly with time t:

$$r(t) = at \tag{1}$$

where a is an arbitrary constant. It follows that

$$\frac{dr}{dt} = a \tag{2}$$

Ultimately, we are interested in how the volume changes over time ($\frac{dV}{dt}$) to be able to compare it with known growth models. We can calculate $\frac{dV}{dt}$ with the help of the known $\frac{dr}{dt}$ by:

$$\frac{dV}{dt} = \frac{dr}{dt}\frac{dV}{dr} \tag{3}$$

The volume and the radius are related by the formula for the volume of a sphere $V = \frac{4}{3}\pi r^3$. Calculating the derivative of the volume with respect to the radius

$$\frac{dV}{dr} = 4\pi r^2 = A \tag{4}$$

results in the expression for the surface area A of a sphere. Using equations (2) and (4) in (3) leads to

$$\frac{dV}{dt} = aA \tag{5}$$

This shows that if the radius grows linearly with time, the volume always grows proportionally to the surface area. Using the formulas for the surface area and the volume of a sphere, we see that plotting surface area over time would result in a quadratic curve, while the volume depends on time to the power of 3.

1.2 Growth proportional to volume

For comparison, we briefly describe what growth proportional to the volume would look like. Growth proportional to volume means that

$$\frac{dV}{dt} = aV \tag{6}$$

Solving this leads to

$$logV = at + C \tag{7}$$

where C is an arbitrary constant. Using the formula for the volume of a sphere, we can express the volume as a function of the radius:

$$log\left(\frac{4}{3}\pi r^3\right) = at + C \tag{8}$$

This can be rewritten as

$$\frac{4}{3}\pi r^3 = e^{at+C} \tag{9}$$

Solving for r leads to

$$r(t) = \left(\frac{3}{4\pi}\right)^{\frac{1}{3}} e^{\frac{1}{3}(at+C)} \tag{10}$$

This means that r would grow exponentially with time. The same is true for the surface area A and the volume (by using the expression for r in equation (10) in $A = 4\pi r^2$, $V = \frac{4}{3}\pi r^3$).

1.3 Constant growth

Another common model of growth is constant growth with respect to the volume, where

$$\frac{dV}{dt} = a \tag{11}$$

Solving this leads to

$$V = at + C \tag{12}$$

Including the volume as a function of radius

$$\frac{4}{3}\pi r^3 = at + C \tag{13}$$

leads to the following dependence of r on time t:

$$r(t) = \left(\frac{3(at+C)}{4\pi}\right)^{\frac{1}{3}} \tag{14}$$

This shows that in case of constant growth with respect to the volume, the radius would grow proportional to $t^{\frac{1}{3}}$, the surface area proportional to $t^{\frac{2}{3}}$, and the volume (as the name of this model says) proportional to t.